Journal of Nuclear Materials 463 (2015) 246–249

Contents lists available at ScienceDirect

Journal of Nuclear Materials

journal homepage: www.elsevier.com/locate/jnucmat

Theoretical investigation of crack formation in tungsten after heat loads

A.S. Arakcheev [a,b,*,1], A. Huber [c], M. Wirtz [c], G. Sergienko [c], I. Steudel [c], A.V. Burdakov [a,b], J.W. Coenen [c], A. Kreter [c], J. Linke [c], Ph. Mertens [c], A.A. Shoshin [a,b], B. Unterberg [c], A.A. Vasilyev [a,b]

[a] Budker Institute of Nuclear Physics SB RAS, 11, akademika Lavrentieva prospect, Novosibirsk 630090, Russia
[b] Novosibirsk State University, 2, Pirogova str., Novosibirsk 630090, Russia
[c] Institute of Energy and Climate Research, Forschungszentrum Jülich, Assoc. EURATOM-FZJ, D-52425 Jülich, Germany

ARTICLE INFO

Article history:
Available online 6 November 2014

ABSTRACT

Transient events such as ELMs in large plasma devices lead to significant heat load on plasma-facing components (PFCs). ELMs cause mechanical damage of PFCs (e.g. cracks). The cracks appear due to stresses caused by thermal extension. Analytical calculations of the stresses are carried out for tungsten. The model only takes into account the basic features of solid body mechanics without material modifications (e.g. fatigue or recrystallization). The numerical results of the model demonstrate good agreement with experimental data obtained at the JUDITH-1, PSI-2 and GOL-3 facilities.

1. Introduction

Operation of magnetic plasma confinement devices for realization of controlled thermonuclear synthesis is accompanied by high-power plasma flow out of the vessel. The interaction of the plasma with the device constructions leads to both material destruction and degradation of plasma parameters. There is an important threshold of plasma flow intensity associated with exceeding of the melting temperature. The exceeding results in great intensification of the mass transport. However, there are phenomena different from surface erosion that are observed even before the threshold. Thus a net of cracks appears on the tungsten surface without melting. The theoretical investigation of the phenomena is the object of the paper.

The observed typical length of the cracks is about the size of the irradiated surface, which is evidence that the local plasma-material interaction is not an immediate cause of the crack formation. The actual reason must be the global mechanical stresses caused by the thermal extension. The features of the plasma-material interaction can influence the characteristics of crack formation (threshold, crack geometry characteristics, etc.) and they should be examined against the background of crack formation due to mechanical stresses. So the calculation of mechanical stresses caused by plasma load and analysis of the crack formation possibility they induce should be carried out. The model that will be discussed can be applied to a variety of materials. However, we will focus on the properties of tungsten, as it is considered to be one of the most promising materials for the divertors of fusion reactors.

2. Stress calculations

2.1. Elastic deformation

First of all let us calculate the elastic stresses. They can be expressed as a function of temperature distribution.

We will not take irradiation nonuniformity into account. This means we will find elastic stresses in a half-space for temperature distribution depending only on distance from irradiated surface. The simplification should not change the answer dramatically because the most intense crack formation is usually observed in the central region of irradiated area.

Let us formulate the problem mathematically.

We will use a rectangular coordinate system with axis z normal to the surface and axes x and y along it. The half-space is situated on the positive z side.

The deformation is described by the equation of mechanical equilibrium [1]:

$$\frac{\partial \sigma_{ij}}{\partial x_j} = 0, \tag{1}$$

where σ_{ik} is the stress tensor, and the forceless boundary conditions are as follows [1]:

$$\sigma_{iz} = 0, \text{ at } z = 0, \tag{2}$$

$$\sigma_{ij} \to 0, \text{ at } z \to \infty. \tag{3}$$

Hook's law is necessary for the solution [1]:

* Corresponding author at: 11, akademika Lavrentieva prospect, Novosibirsk 630090, Russia.
E-mail address: asarakcheev@gmail.com (A.S. Arakcheev).
[1] Presenting author.

http://dx.doi.org/10.1016/j.jnucmat.2014.10.090
0022-3115/

$$\sigma_{ij} = E\left(\frac{1}{1+\sigma}u_{ij} + \frac{\sigma}{(1+\sigma)(1-2\sigma)}u_{ll}\delta_{ij}\right) - \frac{\alpha E}{1-2\sigma}(T-T_0)\delta_{ij}, \quad (4)$$

where E is Young's modulus; σ is Poisson's ratio; u_{ij} is the deformation tensor; α is the linear coefficient of thermal expansion; T is the temperature field; T_0 is the initial (or base) temperature of the material. The tensor indexes take on values "x", "y" or "z". The stress tensor is symmetric and consequently contains 6 independent components, which define the state of stress at a point inside the material.

There is an exact solution of the problem:

$$\sigma^e_{zz} = \sigma^e_{xy} = \sigma^e_{xz} = \sigma^e_{yz} = 0, \quad (5)$$

$$\sigma^e_{xx} = \sigma^e_{yy} = -\frac{\alpha E(T(z)-T_0)}{(1-\sigma)}. \quad (6)$$

These expressions have an important feature of the stress dependence on the local temperature only.

The approximate expressions can be applied only if the heated area thickness is small as compared with its size along the surface and the material thickness. The latter conditions are fulfilled for transient events in plasma devices. The model gives zero stresses for "cold" layers of the material where there must be some small stresses. It can result in underestimation of the crack depth.

The solution provides a simple physical interpretation: each layer of the material experiences thermal extension, but cold layers prevent its expansion along the surface. As a result, there appear stresses along the surface. The interpretation enables due account of the dependence of all mechanical parameters on temperature.

2.2. Plastic deformation

Plastic deformation depends on the history of influences and cannot be expressed as a function of temperature distribution. Thus it is necessary to formulate a model of plastic deformation and specify the time dependence of the temperature. Let us discuss the plastic deformation.

The plastic behavior of tungsten has a key feature of high ductile-to-brittle transition temperature (DBTT). The DBTT of pure tungsten is in the interval of 200–400 °C [2]. To take it into account, we apply two models: a brittle body at temperature below the DBTT and a ductile one otherwise (Fig. 1).

In the ductile body, stresses greater than certain values result in plastic deformations. In case of stresses expressed by (5) and (6) the plastic deformation begins at stresses along the surface equal to the yield strength (σ_y). The plastic deformation is directed like the elastic one and leads to a reduction in the stresses to the yield strength. The hardening can be neglected because the amplitude of tungsten deformation caused by thermal expansion is strongly limited (about 2 percent elongation for heating from the room temperature to the melting one).

The plastic deformation of the material generates displacements without residual stresses. This should be expressed as an additional part of the deformation tensor in Hook's law. The new summand can be represented as a "plastic stress tensor". The approach works for constant mechanical properties (Young's modulus and Poisson's ratio). We will use it for tungsten due to the quite little temperature range significant for crack formation (between the initial temperature and the DBTT). So the complete stress is a sum of elastic and plastic ones:

$$\sigma_{ij} = \sigma^e_{ij} + \sigma^p_{ij}. \quad (7)$$

Plastic deformation is impracticable with a brittle body. So we will suppose the plastic stresses are constant at temperatures below the DBTT. The condition of crack formation in brittle material is that the complete stress reaches the ultimate tensile strength (σ_t).

2.3. Time dependence

The dependence of the elastic stresses on temperature is local. Consequently, the plastic ones depend only on the history of local temperature, and the stresses can be calculated independently at each layer of the material under the surface. To determine the conditions of crack formation, let us examine the time dependence of the stresses at a certain depth. Fig. 2 illustrates the derivation of the conditions.

We need to specify the time dependence of temperature at the depth. Let us use the simplest variant: the temperature of layer increases from the initial temperature T_0 to a certain maximum one T_{max} and then goes back down. The elastic stress is proportional to the temperature rise as in expression (6). The behavior of the plastic and complete stresses consists of five stages denoted in Fig. 2.

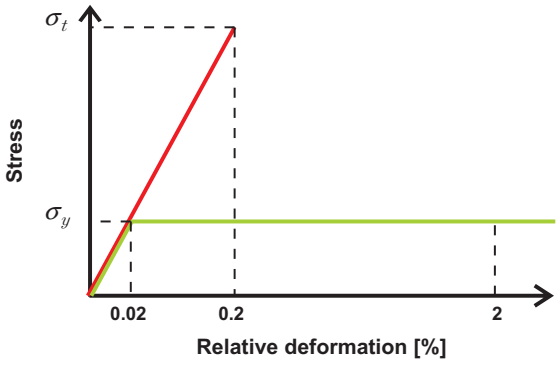

Fig. 1. Deformation curves. The red line corresponds to the brittle body, and the green one to the ductile body. The typical values of deformation are specified for tungsten. 2% is the maximum deformation caused by thermal expansion. (For interpretation of the references to color in this figure legend, the reader is referred to the web version of this article.)

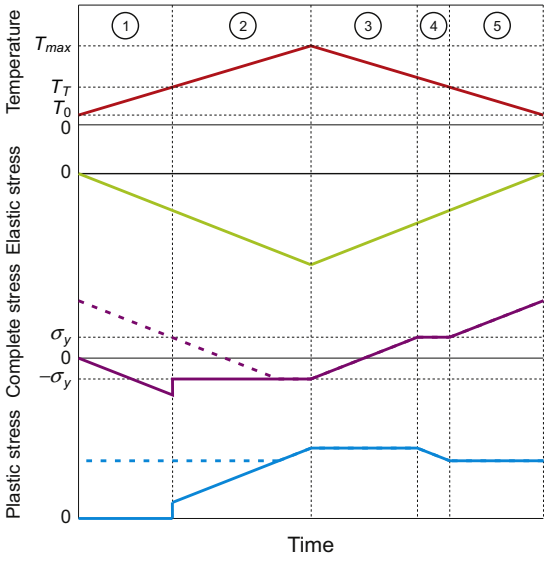

Fig. 2. Schematic development of temperature and elastic, plastic and complete stresses along surface during heating and cooling. The graphs are drawn without respect to actual scales of temperature, stress and time. The solid line corresponds to the first heating–cooling cycle; the dashed line presents the modification in the second and subsequent cycles.

At the first stage the temperature increases and reaches the DBTT. The latter is the first condition of the crack formation:

$$T_{\max} > T_T, \tag{8}$$

where T_T is the DBTT. The second stage begins with exceeding of the DBTT. Complete stress in a ductile material cannot exceed the yield strength. Thus a plastic deformation takes place with tensile plastic stress formation (a positive stress). The plastic stress increases together with temperature and reaches the maximum value at the end of the second stage:

$$\sigma^p_{xx} = \sigma^p_{yy} = \frac{\alpha E}{1-\sigma}(T_{max} - T_0) - \sigma_y. \tag{9}$$

The tensile plastic stress causes crack formation when the temperature returns to the initial value. Thus the maximum value of the plastic stress must exceed the ultimate tensile strength. It is the second condition of crack formation:

$$\frac{\alpha E}{1-\sigma}(T_{max} - T_0) - \sigma_y > \sigma_t. \tag{10}$$

At the third stage the elastic stress and the temperature begin decreasing in absolute value. The plastic stress does not change, because the complete stress is less than the yield strength. During this stage the complete stress reverses its sign. At the fourth stage the reversed complete stress causes opposite plastic deformation, reducing the plastic stress. The fifth stage begins when the temperature becomes lower than the DBTT. The complete stress rises above the yield strength in the brittle material. The final complete stress consists only of plastic part and equals to the yield strength plus the stress corresponding to the temperature difference between the DBTT and the initial temperature:

$$\sigma_{xx} = \sigma_{yy} = \sigma_y + \frac{\alpha E}{1-\sigma}(T_T - T_0). \tag{11}$$

Cracks form if the stress is larger than the ultimate tensile stress. The third condition of crack formation is

$$T_0 < T_T - \frac{1-\sigma}{\alpha E}(\sigma_t - \sigma_y). \tag{12}$$

The three conditions of crack formation does not change for the second and next heating–cooling cycles if we do not consider modification of material (fatigue, recrystallization, etc.). The modifications can be taken into account due to known mechanical and thermal states of material (see Fig. 2).

3. Comparison with experimental results

3.1. Conditions of crack formation

The three obtained conditions of crack formation (8), (10) and (12) contain two variables depending on the irradiation parameters T_0 and T_{max}. The former can be easily measured or estimated. The latter may be calculated on the basis of the heating power and its distribution under the surface. We compared the theoretical prediction with experimental results of three facilities: JUDITH-1 (Jülich), PSI-2 (Jülich) and GOL-3 (Novosibirsk). The facilities use different methods of simulation of plasma load: electron beam, laser and hot plasma flow with relativistic electron beam. At JUDITH-1 and PSI-2 the energy is released in a thin surface layer [3,4]. So we will simulate the heat load by surface heating. The maximum temperature for constant heating power occurs at the surface and is expressed by the following formula:

$$T_{max} = T_0 + 2\sqrt{\frac{\tau}{\pi C_P D}}W, \tag{13}$$

where τ is the duration of irradiation; C_P is the specific volumetric thermal capacity; D is the heat conductivity and W is the density of surface power. At GOL-3, high-energy electrons provide a deep energy release [5,6]. In tungsten, 1 MeV electrons give a penetration depth of about 400 μm. With a 10 μs exposure the heat does not has time to diffuse from the release place. So the temperature after

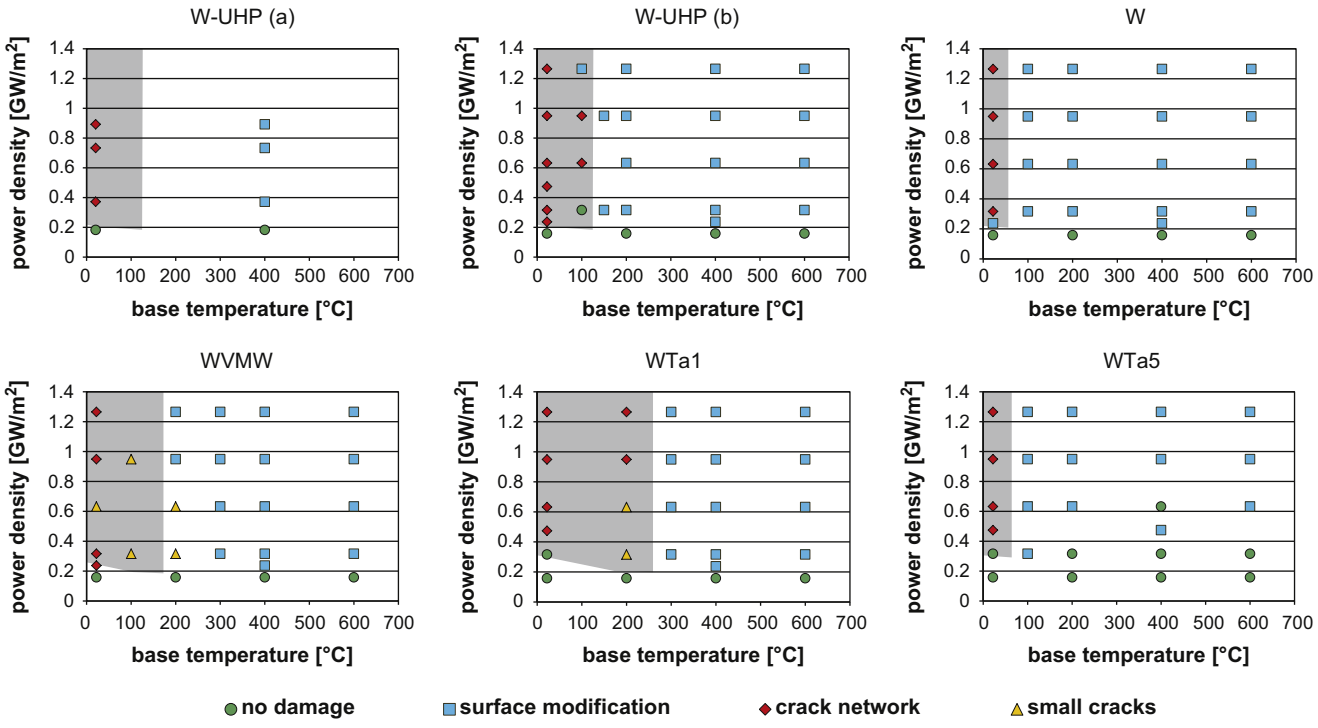

Fig. 3. Results of tungsten irradiation are presented in the coordinates of base temperature and power density. The gray background corresponds to the theoretically predicted area of crack formation. The experimental results after a hundred of 1-ms pulses are presented by the shapes and colors of the points (see the legend under the graphs). The W-UHP results (a) were obtained at PSI-2; the other at JUDITH-1. Descriptions of the experiments have been published in detail [3,7,10]. (For interpretation of the references to color in this figure legend, the reader is referred to the web version of this article.)

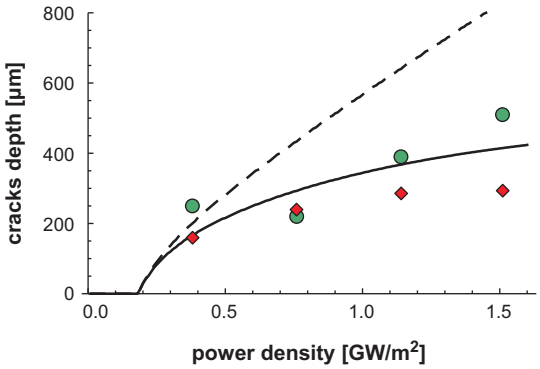

Fig. 4. Crack depth versus heating power density. Red diamonds – electron beam at JUDITH-1, green circles – laser irradiation at PSI-2, dashed line – one-dimensional calculation, solid line – corrected calculation ($r \approx 1$ mm). Descriptions of the experiments have been published in detail [7,10]. (For interpretation of the references to color in this figure legend, the reader is referred to the web version of this article.)

irradiation can be estimated as local density of volume heating divided by specific thermal capacity.

The methods permit transition from maximum temperature to surface power in the conditions of crack formation and their comparison with the experimental results. Such comparison for JUDITH-1 and PSI-2 is presented in Fig. 3. Five materials were irradiated: ultra high purity tungsten (W-UHP), pure tungsten (W), Vacuum-Metallizing-Tungsten (WVMW) and alloys consisting of pure tungsten with 1 and 5 wt% tantalum (WTa1 and WTa5).

The data on Young's modulus, heat conductivity, coefficient of thermal expansion and specific thermal capacity are taken from work [7]. The ultimate tensile strengths were obtained by interpolation of maximum achievable stress as a function of temperature. We used Poisson's ratio for tungsten ($\sigma = 0.29$) [2] and annealed tungsten yield strength for all materials. The DBTTs are fitted for better coincidence. The final values are as follows: W-UHP – 320 °C, W – 300 °C, WVMW – 400 °C, WTa1 – 500 °C, WTa5 – 500 °C.

The experiments at GOL-3 were carried out with rolled tungsten. The grains were oriented along the surface. Thus the cracks were also oriented. However the presence of the preferential direction along the surface cannot dramatically change the conditions of crack formation. The experiments at GOL-3 are carried out with significant exceeding of the crack formation power threshold described by expressions (8) and (10). Therefore only the third condition of crack formation (12) could be checked. There is no accurate data on the properties of the material used. So, to see the difference, we carried out the experiments at the initial room temperature and at 500 °C. Detailed descriptions of the experiments are under publishing [8,9]. The cracks were obtained only in the first case, which is in agreement with the presented model.

3.2. Depth of cracks

The conditions of crack formation can be applied to each layer of material under the surface. The obtained conditions of crack formation (8), (10) and (12) contain only one parameter depending on irradiation – the maximum temperature of the layer. This means that a crack forms if the maximum temperature exceeds a certain value $\left(T^* = T_0 + \frac{1-\sigma}{\alpha E}(\sigma_t + \sigma_y)\right)$. Note that the method is a lower estimation due to incorrectness of expressions (5) and (6) after crack formation.

The one-dimensional temperature distribution was calculated numerically using an explicit difference scheme for surface heating relevant to experiments at JUDITH-1 and PSI-2. The time dependence of temperature distribution gives the maximum temperature as a function of depth. The depth at which the function value equals T^* corresponds to the crack depth. The derived crack depth dependence on heating power ($h(W)$) is compared with the experimental data (see Fig. 4) [10]. The maximum crack depth is about the size of the irradiated area. Thus we had to use a rough allowance for the three-dimensional temperature propagation. With three-dimensional temperature propagation, the heat diffuses not only inside the material but also along the surface. As the total energy is fixed, the volume heated to a certain temperature is almost the same. Thus the depth of the layer with the maximum temperature T^* should decrease proportionally to the heated area. For one-dimensional temperature propagation, the heated area coincides with the loaded area. Let us denote its radial size r. The distance of temperature propagation may be estimated as the uncorrected crack depth. So, for three-dimensional temperature propagation, the radial size of the heated area is about $r + h$. Thus we obtained an expression for the corrected crack depth:

$$h_c = h\frac{r^2}{(r+h)^2}, \tag{14}$$

where h_c is the corrected crack depth and r is a coefficient close to the radial size of the loaded area. The corrected and experimental data are compared in Fig. 4.

4. Conclusion

Heating is the only aspect of external action on material taken into account in the presented model. The basic features of deformable body mechanics explain appearance of tensile plastic stress after a heating–cooling cycle. The mechanical stresses are calculated under an assumption of smallness of the heated area thickness in comparison with its size along the surface and material thickness. Besides, material modifications (fatigue, recrystallization, etc.) are not necessary for achievement of quite good qualitative and quantitative agreement in theoretical calculations and experimental data for different kinds of influence on material (laser, electron beam and plasma flow). It suggests that heating and its distribution are main parameters of the plasma influence on material and define the crack formation in a low-cycle pulse load.

Acknowledgements

The work was partially financially supported by RFBR Grant 14-08-01037 and the State through the Ministry of Education and Science of Russia (Project RFMEFI61914X0003).

The authors are grateful to I.G. Sokolova and A.V. Sorokin.

References

[1] L.D. Landau, E.M. Lifshitz, Theory of elasticity, A Course of Theoretical Physics, vol. 7, Pergamon Press, 1970.
[2] I. Smid, M. Akiba, et al., J. Nucl. Mater. 258–263 (1998) 160–172.
[3] M. Wirtz, J. Linke, et al., J. Nucl. Mater. 438 (2013) S833–S836.
[4] A. Huber, A. Arakcheev, et al., Phys. Scr. T159 (2014) 014005.
[5] A.V. Arzhannikov, V.A. Bataev, et al., J. Nucl. Mater. 438 (2013) S677–S680.
[6] A.A. Shoshin, A.V. Arzhannikov, et al., Fusion Sci. Technol. 59, 1T (2011) 57–60.
[7] O.M. Wirtz, Thermal shock behaviour of different tungsten grades under varying conditions, Schriften des Forschungszentrums Jülich, Reihe Energie und Umwelt/energy and Environment, vol. 161, Forschungszentrum, Zentralbibliothek, 2013, ISBN 9783893368426, p. 14. 130 S.
[8] A.A. Shoshin, A.S. Arakcheev, et al., in: 21st International Conference on Plasma Surface Interactions in Controlled Fusion Devices, Kanazawa, Japan, 26–30 May 2014, P3-035.
[9] A.A. Shoshin, A.S. Arakcheev, et al., in: Abstracts of 10th Intern. Conf. on Open Magnetic Systems for Plasma Confinement, Daejeon, Korea, 26–29 August 2014.
[10] A. Huber, A. Burdakov, et al., Fusion Sci. Technol. 63 (1T) (2013) 197–200.